

1 **Combining biorelevant *in vitro* and *in silico* tools to simulate and better understand the *in vivo***
2 **performance of a nano-sized formulation of aprepitant in the fasted and fed states.**

3

4 Chara Litou¹, Nikunj Kumar Patel², David B. Turner², Edmund Kostewicz¹, Martin Kuentz³, Karl J. Box⁴,
5 Jennifer Dressman^{1*}

6 ¹Institute of Pharmaceutical Technology, Goethe University, Frankfurt am Main, Germany

7 ²Certara UK Limited, Simcyp Division, Level 2-Acero, 1 Concourse Way, Sheffield, S1 2BJ, UK

8 ³University of Applied Sciences and Arts Northwestern Switzerland, Gründenstr. 40, 4132, Switzerland

9 ⁴Pion Inc. (UK) Ltd., Forest Row, East Sussex, UK

10

11

12 Running Title: PBPK modeling of aprepitant in the fasted and fed state

13

14 *To whom correspondence should be addressed:

15 **Prof. Dr. Jennifer Dressman, Institute of Pharmaceutical Technology, Biocenter, Johann Wolfgang**

16 **Goethe University, Max-von-Laue-Str. 9, 60438 Frankfurt am Main, Germany.**

17 **E-mail: dressman@em.uni-frankfurt.de**

18 **ABSTRACT**

19 **Introduction:** When developing bio-enabling formulations, innovative tools are required to understand
20 and predict *in vivo* performance and may facilitate approval by regulatory authorities. EMEND® is an
21 example of such a formulation, in which the active pharmaceutical ingredient, aprepitant, is nano-sized.
22 The aims of this study were 1) to characterize the 80 mg and 125 mg EMEND® capsules *in vitro* using
23 biorelevant tools, 2) to develop and parameterize a physiologically based pharmacokinetic (PBPK)
24 model to simulate and better understand the *in vivo* performance of EMEND® capsules and 3) to assess
25 which parameters primarily influence the *in vivo* performance of this formulation across the
26 therapeutic dose range.

27 **Methods:** Solubility, dissolution and transfer experiments were performed in various biorelevant media
28 simulating the fasted and fed state environment in the gastrointestinal tract. An *in silico* PBPK model for
29 healthy volunteers was developed in the Simcyp Simulator, informed by the *in vitro* results and data
30 available from the literature.

31 **Results:** *In vitro* experiments indicated a large effect of native surfactants on the solubility of aprepitant.
32 Coupling the *in vitro* results with the PBPK model led to an appropriate simulation of aprepitant plasma
33 concentrations after administration of 80 mg and 125 mg EMEND® capsules in both the fasted and fed
34 states. Parameter Sensitivity Analysis (PSA) was conducted to investigate the effect of several parameters
35 on the *in vivo* performance of EMEND®. While nano-sizing aprepitant improves its *in vivo* performance,
36 intestinal solubility remains a barrier to its bioavailability and thus aprepitant should be classified as DCS
37 IIb.

38 **Conclusions:** The present study underlines the importance of combining *in vitro* and *in silico*
39 biopharmaceutical tools to understand and predict the absorption of this poorly soluble compound from
40 an enabling formulation. The approach can be applied to other poorly soluble compounds to support

41 rational formulation design and to facilitate regulatory assessment of the bio-performance of enabling
42 formulations.

43 **KEYWORDS**

44 PBPK, modeling and simulation, nano-sized drugs, bio-enabling formulations, aprepitant

45 1. Introduction

46 In recent years there has been increasing interest from various regulatory authorities in facilitating earlier
47 access to innovative medicines, without compromising their safety and/or efficacy. Indeed, EMA and FDA
48 have taken initiatives to accelerate the approval of innovative medicines which address unmet medical
49 needs.^[1-3] On the other hand, the development of new drug products has become more demanding due
50 to the implementation of stricter safety and quality requirements.^[4] Contributing further to long
51 development times are the increasingly challenging properties of new active pharmaceutical ingredients
52 (APIs), which make formulation development more difficult and pose a significant barrier to drug
53 absorption and clinical efficacy. Indeed, although about 40% of APIs in marketed drug products exhibit
54 poor solubility and/or permeability, almost 90% of APIs in early drug development stages are saddled
55 with these undesirable characteristics.^[5,6] In response to these issues, the European Research Program
56 “PEARRL” (www.pearrl.eu) aims to 1) develop creative bio-enabling formulations, 2) establish, validate
57 and optimize innovative biopharmaceutical *in vitro* tools and 3) understand and predict the *in vivo*
58 behavior of various drug products with physiologically-based pharmacokinetic (PBPK) modeling and
59 simulation.

60 As part of the PEARRL consortium, the present research aims to link the results obtained using biorelevant
61 *in vitro* tools with *in silico* PBPK models to simulate and better understand the *in vivo* performance of the
62 marketed formulation of aprepitant in the fasted and fed states. Aprepitant is a selective substance P
63 neurokinin (NK1) receptor antagonist which, in combination with other antiemetic agents, is indicated
64 for the prevention of both acute and delayed nausea and vomiting associated with emetogenic cancer
65 chemotherapy.^[7,8] It is available as oral capsules (40, 80 and 125 mg), under the brand name EMEND®
66 (reference listed product) and as a water soluble prodrug form, fosaprepitant dimeglumine, for
67 intravenous administration (EMEND® for injection).^[7] For ambulant therapy, EMEND® is administered for

68 three days with a recommended dosing regimen of 125 mg orally once on Day 1 and 80 mg orally once
69 daily on Days 2 and 3.^[7]

70 Aprepitant has both very weak acidic and very weak basic properties and possesses a logD of 4.8 at pH
71 7.0.^[9-13] According to Wu et al.,^[11] it exhibits very low aqueous solubility (3-7 µg/mL over the pH range 2-
72 10), although solubilities of just 0.37 µg/mL and 0.8 µg/mL in phosphate buffers at pH 6.5 were reported
73 by Söderlind et al. and Takano et al., respectively.^[14,15] In line with the expected protonation behavior,
74 Niederquell and Kuentz recently concluded that aprepitant acts like a neutral compound at small
75 intestinal pH.^[16] Concurrently, solubility values of 13 µg/mL in Human Intestinal Fluids (HIF)^[14] and of 21
76 µg/mL in media simulating the canine fasted small intestine [FaSSIF_{dog}, 5mM sodium taurocholate (NaTc),
77 1.25 mM lecithin]^[15] have been reported, suggesting a pronounced effect of native surfactants on the
78 solubility of aprepitant.

79 With regard to the permeability of aprepitant, a wide range of permeability values from Caco-2 assays
80 has been reported in the open literature, including a P_{app} of 7.8×10^{-6} cm/s (no reference substance value
81 provided),^[10,11] a P_{app} of 170×10^{-6} cm/s (no reference substance value provided),^[13] or a P_{app} of 21×10^{-6}
82 cm/s with metoprolol as a reference compound ($P_{app} = 5 \times 10^{-6}$ cm/s)^[15]. Due to its permeability and
83 solubility properties, aprepitant has been classified as a borderline BCS II/IV compound.^[9,10]

84 The aprepitant tablet formulations used in the early clinical phases exhibited high variability and a large
85 food effect on absorption. Considering the target patient group addressed by aprepitant (cancer patients
86 suffering from nausea and vomiting), administration with food was deemed unacceptable and, therefore,
87 the next formulation efforts were focused on attenuating the food effect and improving dissolution
88 characteristics. This was accomplished by decreasing the particle size to the nanoscale range (approx.
89 200 nm).^[7,17] As illustrated e.g. by the study of Shono et al.,^[9] nano-sizing aprepitant proved to be a
90 successful strategy for reducing the food effect over the clinical dose range.^[17] After administration of
91 the EMEND® 80 mg and 125 mg capsules (the currently marketed formulation), the absolute
92 bioavailability under fasting conditions is 67% (62-73%) and 59% (53-65%), respectively. In the

93 therapeutic dose range a standard breakfast results in a mild increase in bioavailability (the geometric
94 means AUC_{fed}/AUC_{fasted} for the 125 mg and 80 mg dose are reported to be 1.20 and 1.09, respectively),
95 but this is not considered clinically relevant.^[7,17,18]

96 The aims of this study were threefold: 1) to investigate the advantages of using biorelevant media vs.
97 simple buffers in simulating the *in vivo* performance of aprepitant, 2) to build a PBPK model following the
98 “middle-out” approach, combining experimental data and information available in literature with the
99 commercially available *in silico* software Simcyp Simulator V16.1 (Certara UK Ltd.) and 3) to
100 mechanistically understand the *in vivo* behavior of aprepitant in both the fasted and fed states.

101 **2. Materials and Methods**

102 *2.1 Chemicals and reagents*

103 Aprepitant was obtained as the European Pharmacopeia reference standard (code: Y0001825).
104 Acetonitrile and water of HPLC-grade were from Merck KGaA (Darmstadt, Germany). Sodium dihydrogen
105 phosphate dihydrate of analytical grade was from Merck KGaA (Darmstadt, Germany). Phosphoric acid,
106 sodium chloride and sodium hydroxide, also of analytical grade, were purchased from VWR chemicals
107 (Leuven, Belgium). Pepsin was from Sigma-Aldrich (Lot # SLBQ2263V). EMEND® capsules were purchased
108 from MSD SHARP & DOHME GMBH (Lot # MO 49340 and MO 45740 for the 80 mg and 125 mg,
109 respectively, Haar, Germany). Lipofundin® MCT/LCT 20% was purchased from B. Braun (B. Braun
110 Melsungen AG, Melsungen, Germany). FaSSGF/FaSSIF/FeSSIF, FeSSIF V2 and FaSSIF V3 powders were
111 kindly donated by biorelevant.com (London, England).

112 *2.2 Experimental Methods*

113 2.2.1 Solubility experiments

114 The solubility of pure aprepitant powder was investigated using the method of Andreas et al.^[19] in Level
115 I and Level II biorelevant media,^[20] utilizing the Uniprep™ system (Whatman®, Piscataway, NJ, USA).
116 Briefly, an excess amount of aprepitant is added to a 3 mL aliquot of the medium and the samples are
117 shaken for 1, 2, 4, 24 or 48 h at 37 °C on an orbital mixer. After shaking, the samples are immediately
118 filtered through pre-warmed 0.45 µm PTFE filters and analyzed by HPLC. Solubility measurements were
119 carried out at least in triplicate (n=3).

120 2.2.2 Dissolution experiments

121 Dissolution experiments of the EMEND® capsules were performed using the paddle (USP II) apparatus
122 (Erweka DT 600, Heusenstamm, Germany). Each vessel contained 250 mL or 500 mL, respectively, for
123 media simulating gastric fluids or intestinal fluids. The rotating speed of the paddle was set at 75 rpm.

124 The temperature in the vessels was maintained at 37 ± 0.5 °C throughout the experiment. All dissolution
125 experiments were performed in triplicate (n=3).

126 Samples were withdrawn at 1, 2.5, 5, 7.5, 10, 20, 30, 40, 60, 90 and 120 min with glass syringes and
127 filtered through a cylindrical polyethylene filter stick with a pore size of 4 µm attached to the end of the
128 sampling tubes. Immediately thereafter, the samples were filtered through 0.1 µm Anotop 25 filters
129 (Whatman GmbH, Dassel, Germany). After discarding the first 1 mL, the filtrate was diluted with mobile
130 phase and analyzed by HPLC.

131 The efficiency of filtration was confirmed with Nanoparticle Tracking Analysis (NTA) on a Malvern
132 Nanosight NS300 (Malvern Instruments, Malvern, UK) instrument that was equipped with a green laser
133 (excitation at 468 nm, emission at 508 nm).

134 2.2.3 Transfer experiments

135 Transfer experiments were performed for both the 80 mg and 125 mg EMEND® capsules utilizing the USP
136 II apparatus, as described previously by Berlin et al.^[21] Briefly, 250 mL of Level III FaSSGF pH 2.0 and 350
137 mL of Level II FaSSIF V1 or FaSSIF V3 were used as the dissolution media in the gastric and duodenal
138 compartment, respectively. The rotating speed of the paddles was set at 75 rpm. The temperature in the
139 vessels was maintained at 37 ± 0.5 °C throughout the experiment. A peristaltic pump set to first order
140 kinetics ($t_{1/2} = 9$ min) was used to transfer the dissolved drug from the gastric to the duodenal
141 compartment, from which samples were withdrawn at 5, 10, 15, 20, 30, 45, 60, 75, 90, 120, 180 and 240
142 min. Sample handling and analysis were as described for the dissolution experiments.

143 2.2.4 Chromatographic assays

144 For the quantitative analysis of samples, a HPLC-UV system was used (Hitachi Chromaster; Hitachi Ltd.,
145 Tokyo, Japan or Spectra System HPLC, ThermoQuest Inc., San Jose, USA). The analytical column was a
146 BDS Hypersil C18, 3µm, 150 x 3mm (Thermo Scientific) combined with a pre-column (BDS Hypersil C-18,
147 3µm, 10 x 4mm). The mobile phase consisted of 50:50 % v/v buffer (NaH_2PO_4 , 10mM, pH=2.5) :

148 acetonitrile. The detection wavelength was set at 220 nm, the injection volume at 50 μ L and the flow rate
149 at 1 mL/min. The LOD (limit of detection) and LOQ (limit of quantification) were 0.02 μ g/mL and 0.07
150 μ g/mL, respectively.

151 *2.3 Pharmacokinetic data and methods*

152 2.3.1 Literature pharmacokinetic data

153 In order to build the PBPK model for aprepitant following the “middle-out” approach,^[22,23] plasma data
154 for both dose strengths for fasted and fed state were derived from the study of Majumdar et al. and
155 digitalized with WebPlotDigitizer v. 4.0, Texas, USA.^[18] The study reported by Majumdar et al. consisted
156 of two parts. The first part was a single-period, double blind study, in which 2 mg of aprepitant were
157 intravenously administered to nine healthy volunteers (mean age was 31 years with a range of 24-40).
158 The second part was a randomized, four period, cross-over study with the aim of investigating the
159 absolute bioavailability of the 80 mg and 125 mg EMEND® capsules under fasted and fed state conditions.
160 In this part of the study, twenty-five healthy volunteers (mean age was 28 years with a range of 18-43)
161 were administered: 1) one aprepitant 80 mg capsule orally following a standard breakfast, 2) one
162 aprepitant 125 mg capsule orally following a standard breakfast, 3) one aprepitant 80 mg capsule orally
163 with 8 oz. of water, along with 2 mg intravenous, isotope-labeled aprepitant, and 4) one aprepitant 125
164 mg capsule orally with 8 oz. of water, along with 2 mg intravenous, isotope-labeled aprepitant. The
165 authors commented that the co-administration of the 2 mg intravenous isotope-labeled aprepitant had
166 little effect on the disposition of the drug relative to the 80 mg and 125 mg capsules. Since there were
167 earlier data demonstrating non-linearity of the pharmacokinetics of aprepitant with increasing dose, the
168 bioavailability of the capsule formulations was determined by comparing the dose-standardized AUC
169 values following the capsule dose to the dose-standardized AUC values following the capsule dose
170 simultaneously administered with 2mg intravenous, isotope-labeled aprepitant.^[17,18]

171 2.3.2 Modeling methods and strategies

172 The *in vivo* performance of aprepitant capsules was modeled with the Simcyp Simulator V16.1 (Certara
173 UK Ltd., Sheffield, UK). The substrate parameters for building the i.v. and/ or oral PBPK model are
174 presented in Table 1.

175 Disposition parameters were calculated from the available i.v. data and the resulting fit of the model to
176 the observed data is shown in Figure 1.^[18] The distribution of aprepitant was described using a minimal
177 PBPK model with a Single Adjusting Compartment (SAC). SAC is a non-physiological compartment that
178 represents a cluster of tissues (excluding the liver and portal vein). It is used to extend the use of minimal
179 PBPK models to APIs with high volumes of distribution, i.e. where the tissue concentration exceeds the
180 blood concentration. The Q_{SAC} (inter-compartment clearance), V_{SAC} (apparent volume associated with the
181 SAC) and V_{ss} (steady state volume of distribution) were estimated using the Parameter Estimation Tool
182 and simultaneous fit of the three intravenous PK profiles available in the open literature.^[18]

183 To model the clearance, the “Enzyme Kinetics” option in Simcyp was chosen since aprepitant exhibits
184 saturable metabolism and non-linear pharmacokinetics. As mentioned in the Public Assessment Report
185 of the EMA and FDA of EMEND® capsules, as well as the research article of Sanchez et al., aprepitant is
186 mainly metabolized by CYP3A4,^[8,24,25] although CYP2C19 and CYP1A2 may also be involved to some
187 extent. The V_{max} (*in vitro* maximum velocity for metabolism of the compound by the given isoform of
188 enzyme) and K_m (*in vitro* Michaelis-Menten constant for metabolism of the compound by the given
189 isoform of enzyme) for CYP3A4 were derived by Sanchez et al.^[24] The f_{umic} (fraction of compound unbound
190 in an *in vitro* microsomal preparation) was predicted using the Simcyp Prediction Toolbox.^[26]
191 Furthermore, as indicated in the EMA scientific discussion document for the approval of EMEND®
192 capsules, after intravenous administration of the radio-labelled prodrug of aprepitant (which is rapidly
193 and completely converted to aprepitant) no unchanged drug is recovered in the urine.^[25,27] Therefore,
194 the renal clearance for aprepitant was set at a minimum value corresponding to the product of plasma f_u
195 (fraction unbound) and urine flow.^[28] This approach is further supported by the fact that impaired renal

196 function does not result in a clinically significant difference in the PK of aprepitant when compared to
197 healthy control subjects and no dose adjustment is required for patients with renal insufficiency, end-
198 stage renal disease or those undergoing hemodialysis.^[8,25,29]

199 To model the absorption process, the Advanced Dissolution, Absorption and Metabolism (ADAM) model
200 was utilized.^[30] The segmental (total) solubility input option was used, based on the maximum
201 concentration measured in the dissolution experiments in each biorelevant medium (Section 3.1).
202 Permeability was estimated by using the Parameter Estimation Tool by fitting the *in vivo* PK data following
203 oral administration in the fasted state (simultaneous fit of PK profiles after administration of 80 mg and
204 125 mg) and was in line with the P_{app} values reported in literature by Shono et al.,^[9] Wu et al.^[11] and
205 Takano et al.^[15]

206 All physiological parameters of the gastrointestinal (GI) tract were maintained at the default values for
207 the healthy volunteer population in the Simcyp Simulator for both the fasted and fed state simulations.

208 *2.4 Statistics*

209 To assess the prediction accuracy, average fold error (AFE) and absolute average fold error (AAFE) were
210 calculated according to the equations published by Obach et al., as also described by Andreas et al.^[31,32]
211 The 95% confidence intervals were calculated with the Simcyp Simulator V16.1

212 **3. Results**

213 *3.1 Experimental part*

214 Solubility experiments

215 Mean solubility values (\pm SD) of pure aprepitant (Form I, most thermodynamically stable polymorph) at
216 24 h in Level I and Level III FaSSGF, Level I and Level II FaSSIF V1 and FaSSIF V3, Level I and Level II FeSSIF
217 V1 and FeSSIF V2 are presented in Table 2, together with the pH value at the end of the solubility
218 experiment (pH_{final}). In every case the pH_{final} was only slightly or not at all different from the initial pH
219 value of the medium.

220 The solubility values obtained in Level II compared with Level I biorelevant media indicate a major impact
221 of native surfactants on the solubility of aprepitant. Similar observations have been reported by Zhou et
222 al. and Niederquell and Kuentz.^[16,33]

223 Dissolution and transfer experiments

224 Dissolution and transfer experiments were performed, as described in sections 2.2.2 and 2.2.3, for
225 EMEND® capsules at both dose strengths in biorelevant media simulating the contents of the fasted
226 stomach (Level III FaSSGF), fasted upper small intestine (Level II FaSSIF V1, Level II FaSSIF V3), fed stomach
227 (Level II FeSSGF_{middle}) and fed upper small intestine (Level II FeSSIF V1, Level II FeSSIF V2).^[20] The mean
228 values of % dissolved with time in fasted and fed state biorelevant media for the 80 mg and 125 mg dose
229 are presented in Figures 2 and 3, respectively.

230 In the case of the USP II dissolution experiments the dissolution was fast, incomplete and reached a
231 plateau value within approximately the first 10 min. Interestingly, the concentrations of dissolved drug
232 in the dissolution vessels exceeded the thermodynamic solubility observed for the pure API in the
233 respective media. In particular, the mean maximum concentrations of dissolved drug in Level III FaSSGF,
234 Level II FaSSIF V1, Level II FaSSIF V3, Level II FeSSGF_{middle}, Level II FeSSIF V1 and Level II FeSSIF V2 were
235 approx. 15 µg/mL, 27 µg/mL and 26 µg/mL, 75 µg/mL, 120 µg/mL and 150 µg/mL respectively, at both
236 doses. These results are consistent with those of Shono et al. and Takano et al.^[9,15]

237 Decreasing the particle size of aprepitant to the nanoscale results in a much higher dissolution rate, which
238 can be attributed to the large increase in surface area and surface energy. As reported by Kesisoglou and
239 Mitra, apart from the increase in the dissolution rate, nano-sizing can also lead to some increase in the
240 apparent solubility of the API, according to the Freundlich-Ostwald equation.^[10] However, the
241 quantitative effect of nano-sizing on saturation solubility remains unclear,^[9,34,35] and it can be assumed
242 that the increase in surface area plays the predominant role in the increase in dissolution rate for

243 nanosized formulations. Additionally, some authors have suggested that apparent increases in solubility
244 that have been reported may be largely due to the use of stabilizers (e.g. surfactants).^[36]
245 With regard to the transfer experiments, no precipitation of aprepitant was observed over the four hour
246 experimental duration. The maximum dissolved concentration was achieved more slowly than in the
247 dissolution experiments, since the appearance of the drug in the intestinal compartment is limited by the
248 rate of transfer from the compartment representing the stomach to the one representing the small
249 intestine. Additionally, the maximum dissolved concentration and plateau values achieved in the transfer
250 experiments were somewhat lower than those of the dissolution experiments in media simulating the
251 fasted upper small intestine. This is attributable to the dilution of the intestinal compartment by fluid
252 transferred from the gastric compartment. The results of the transfer experiments with the 80 mg and
253 125 mg doses are presented in Figure 4.

254 *3.2 PBPK model and simulations*

255 Initially, modeling and simulation of the *in vivo* intravenous (i.v.) data was performed to estimate the
256 post-absorptive parameters, as described in 2.3.2. The PBPK model for oral administration of aprepitant
257 was then built using the “middle-out” approach. This entailed implementation of (i) the calculated post-
258 absorptive parameters from the i.v. data together with (ii) results from the *in vitro* dissolution
259 experiments to simulate the plasma profiles. These simulated plasma profiles were then compared with
260 data obtained by Majumdar et al. after oral administration of 80 mg or 125 mg EMEND® capsules in
261 healthy volunteers in the fasted and fed states.^[18] Since the results from the transfer experiments
262 indicated no precipitation over a four hour period, there was no need to invoke precipitation in the PBPK
263 simulations.

264 The simulated plasma profiles after i.v. administration of radio-labelled aprepitant, as well as after oral
265 administration of capsules at both dose strengths in fasted and fed states vs. the observed plasma

266 concentrations, are presented in Figures 1, 5 and 6, respectively. The AAFE and AFE for each simulation
267 are presented in Table 3.

268 **4. Discussion**

269 Fasted state

270 The *in vitro* solubility and dissolution experiments suggest that the solubilization of aprepitant by native
271 surfactants is likely one of the major properties affecting the *in vivo* dissolution of aprepitant from the
272 marketed formulation. The solubility experiments performed with the pure API powder exhibited great
273 differences between the solubility values measured in Level I (simple buffers) and Level II (addition of bile
274 salts and lecithin) biorelevant media. For example the solubility in Level I FaSSIF V1 was below the limit
275 of detection (0.02 µg/mL), but in Level II FaSSIF V1 it was 9.87 ± 2.40 µg/mL. From the dissolution
276 experiments performed with the formulated (nano-sized) drug, the importance of surfactants on the
277 plateau value attained is also evident. Illustratively, the plateau value reached in Level II FaSSIF V1,
278 containing 3 mM NaTc, was approximately double the plateau value reached in Level III FaSSGF, which
279 contains only 0.08 mM NaTc. In agreement with these results, Roos et al. recently demonstrated the
280 importance of colloidal structures in increasing the bioavailability of aprepitant from various nano-
281 suspensions in rat intestinal perfusion experiments.^[37]

282 In the present study, dissolution experiments in the Level II biorelevant media proved more useful than
283 the equilibrium solubility experiments for identifying the relevant apparent solubility of the marketed
284 aprepitant formulation. Thus, the experimental results demonstrated not only that the final
285 concentration of aprepitant in the dissolution experiments was well above the equilibrium solubility, but
286 also that application of the plateau values from the dissolution experiments led to a more accurate
287 simulation of the plasma profiles.

288 The role of bile salts in the dissolution and hence bioavailability of EMEND® in the fasted state was further
289 investigated with the Parameter Sensitivity Analysis (PSA) tool. It should be noted that, due to the way

290 the PBPK model was developed for aprepitant, it was not able to account for inter-individual variations
291 in bile salt concentrations, because the “segmental” (total) solubility input option was used (in this case
292 the plateau value from the dissolution experiment). An alternative way to simulate potential effects of
293 inter-subject solubility differences on *in vivo* performance would be to use the estimated micelle-water
294 partition co-efficient ($K_{m:w}$) in the Simcyp Simulator. This would require a precise value of the intrinsic
295 solubility of aprepitant as an input parameter. However, the solubility of aprepitant is a) very small, b) is
296 associated with a relatively large coefficient of variation and c) is not representative of the concentrations
297 achieved in dissolution experiments.

298 Using PSA, the duodenal total solubility value was allowed to range from 10 $\mu\text{g/mL}$ to 90 $\mu\text{g/mL}$, i.e. three
299 times lower and higher than the value experimentally derived from the dissolution experiments and used
300 in the PBPK model for aprepitant in the fasted state (30 $\mu\text{g/mL}$). This range of values for the total solubility
301 reflects the range of bile salt concentrations that has been observed *in vivo* (approx. 2-6 mM in fasted
302 state duodenum and jejunum).^[38,39] The PSA is presented in Figure 7. The results suggest that variations
303 in intestinal bile concentration among individuals would mainly affect C_{max} rather than AUC values.
304 Furthermore, according to the PSA for both the 80 mg dose and 125 mg dose, variations in the observed
305 C_{max} can be explained by differences in bile component concentrations among subjects.

306 The PSA is largely in agreement with conclusions drawn by Shono et al., who identified intestinal solubility
307 as the most important parameter driving the predicted C_{max} in the fasted state.^[9] The results are also in
308 general agreement with the observations of Takano et al., who investigated the rate-limiting step for
309 absorption of various poorly soluble drugs, including aprepitant, in dogs.^[15] In that study it was shown
310 that reducing the particle size of aprepitant below 2 μm produces no further increase in the bioavailability
311 of aprepitant in dogs, even though the dissolution rate continued to increase with particle size reduction.
312 Takano et al.’s study underlined the fact that, for poorly soluble drugs, the rate limiting step to absorption
313 can shift from dissolution to solubility, depending on the formulation strategy adopted.^[15] Taking all of

314 these points into consideration, it seems that aprepitant should be classified as a DCS IIb compound^[40]
315 and that, for fast-dissolving formulations, the *in vivo* solubility is likely to remain a limitation to its *in vivo*
316 performance.

317 Fed state

318 The *in vitro* experiments conducted in biorelevant media simulating the fed state also highlight the
319 importance of surfactants on the apparent solubility of nano-sized aprepitant. For example, the
320 maximum concentration achieved in FeSSIF V1 was more than 4-fold greater than that achieved in FaSSIF
321 V1 (similar to the ratio of NaTc in FeSSIF V1 to FaSSIF V1, which is 15:3). Comparing the plateau values
322 reached in the dissolution experiments in FeSSIF V1 and FeSSIF V2, a slightly higher value (approximately
323 120 µg/mL vs. 150 µg/mL, respectively) was observed in FeSSIF V2. This increase might be due to the
324 additional presence of glyceryl monooleate in FeSSIF V2, which has been found to have a positive
325 solubilization effect on aprepitant powder.^[33]

326 When the PBPK model was adapted to simulate the plasma profile of aprepitant in the fed state, the fits
327 to the observed data were generally very good (AFE and AAFE both less than 1.5). However, the predicted
328 profiles exhibited an earlier t_{max} of about 2 h compared to the clinically observed mean value, i.e. 4 h. We
329 note that the default value for mean gastric residence time in Simcyp is set at one hour, which seems
330 rather short for the fed state. It is believed that in the fed state, liquids and smaller particles (<3–4 mm)
331 such as disintegrated tablets and capsules often empty with food over a time-span which depends largely
332 on the caloric value of the meal.^[41] Thus, the gastric emptying time in the fed state can vary and high
333 caloric meals can result in long gastric emptying times.^[41–45] In the study of Majumdar et al., the EMEND®
334 capsules were administered to the volunteers 15 minutes following a “standard light breakfast”, although
335 no specific information, e.g. the caloric value of the meal, was provided with regard to the nature of the
336 breakfast. According to the information provided in the FDA Public Assessment Report, the effect of food
337 on the performance of EMEND® capsules was investigated after the administration of a meal that “is

338 similar to FDA recommended high-fat, high-calorie breakfast”.^[8] We therefore used the PSA Tool to
339 explore the sensitivity of the simulated pharmacokinetic profiles of the EMEND® capsules in the fed state
340 to the mean gastric residence time (MGRT). Sensitivity analysis was performed by floating the MGRT
341 values over the range of 1 h (default value in Simcyp Simulator) to 4 h (maximum value allowed in Simcyp
342 Simulator). The results of this analysis are presented in Figure 8. Figure 8 indicates that a MGRT greater
343 or equal to 2.5 h would improve the goodness of fit of the simulated profiles. For example, for a MGRT
344 equal to 3 h, the AFE and AAFE for the 80 mg and 125 mg doses would be 1.26 and 1.32, and 1.09 and
345 1.34, respectively.

346 Since aprepitant is characterized as borderline BCS Class II/IV and various permeability values have been
347 reported in the literature, a further PSA was conducted in which the MGRT values were allowed to float
348 over the range 1 h to 4 h and the P_{eff} values were simultaneously allowed to float over the range of 1.16--
349 2.15×10^{-4} cm/s (based on the lowest value reported in literature and the value used in the PBPK model
350 developed, respectively). The results from this additional sensitivity analysis (shown in Figure 9) indicate
351 that, for a mean gastric residence time equal to or greater than 2 h, a relatively small decrease in the
352 permeability would result in a significant prolongation of the predicted t_{max} , without a profound effect on
353 the AUC or C_{max} . For example, if a MGRT of 2.5 h and a P_{eff} of 1.4×10^{-6} cm/s (i.e. 35% smaller value than
354 the one used in the currently developed model) are implemented, the predicted t_{max} increases by 30%,
355 whereas the C_{max} and AUC decrease only by 8.7% and 2.2%, respectively, compared to simulation with a
356 MGRT of 2.5 h and no change in permeability. For this particular example, the AFE and AAFE for the 80
357 mg and 125 mg dose are 1.22 and 1.29, and 1.04 and 1.29, respectively. Therefore, it seems that inter-
358 individual differences in permeability may also affect the absorption of EMEND® in the fed state.

359 Verification of the model and clinical implications

360 Ideally, an appropriate validation of a compound-specific PBPK model would require access to individual
361 *in vivo* data from all clinical trials conducted for the compound. However, in practice, academic scientists

362 usually have to rely on mean plasma profiles, along with their respective variability (if available), or even
363 on single values of summary pharmacokinetic parameters (C_{max} , AUC) reported in the open literature. In
364 order to validate the model presented in this study, simulated plasma profiles or single pharmacokinetic
365 data (C_{max} , t_{max} and AUC values) were compared to information available in the literature. To this end,
366 virtual trials (10 trials, each with 10 volunteers) were performed in the Simcyp Simulator by implementing
367 the PBPK model described in sections 2.3.2 and 3.2. For the fed state model, based on the results of the
368 PSA, a MGRT of 2.5 h was used (instead of 1 h, which is the default value in Simcyp for IR formulations
369 administered in the fed state).

370 Plasma concentration profiles for aprepitant after administration of one 125 mg EMEND® capsule in the
371 fed state in healthy volunteers were reported in the study of Gore et al., 2009.^[46] In the same study, the
372 AUC_{0-24h} and C_{max} values were presented as geometric means together with their respective ranges; AUC_{0-}
373 $_{24h}$ 19456 (15251, 24817) ng·h/mL and C_{max} = 1539 (1229, 1927) ng/mL. Majumdar et al. conducted a
374 second study with the aim of investigating the pharmacokinetic profile during a three-day 125 mg/80 mg
375 aprepitant regimen.^[18] In that study, the volunteers were administered a single oral dose of one 125 mg
376 EMEND® capsule on Day 1 and one 80 mg EMEND® capsule on Days 2 and 3. The doses were administered
377 15 minutes following administration of a light standard breakfast. The mean plasma profile of aprepitant
378 up to the 24th hour (end of Day 1) was used for model evaluation purposes. The data from these studies
379 were digitalized, as described earlier, and compared with the predicted plasma profiles for the 125 mg
380 capsule in the fed state. The results are presented in Figure 10. For both cases the fit was acceptable,
381 with AFE and AAFE less than 1.5.

382 It should be mentioned that a third study, published by Ridhurkar et al., was also identified. This was a
383 bioequivalence study of 125 mg EMEND® capsules after administration of a high-caloric breakfast.^[47]
384 Since the reported pharmacokinetic parameters (mean C_{max} 2304 ng/mL, mean AUC 82997 ng·h/mL,
385 mean t_{max} 7.7 h, $t_{1/2}$ of 25.4 h) were much higher than those of the FDA and EMA Public Assessment

386 Report of EMEND® capsules, or any other comparable clinical study, this study was not considered further
387 for modeling.

388 With regard to cancer patients, who are the patients most often prescribed aprepitant, the EMA Public
389 Assessment Report stated that, based on limited data, the pharmacokinetics of EMEND® capsules in
390 healthy volunteers and patient populations seem to be similar.^[25] That said, the pharmacokinetic studies
391 in cancer populations that have been published to date are not completely consistent with this appraisal.
392 Takahashi et al. investigated the pharmacokinetics of EMEND® as a 125 mg/80 mg three-day dose
393 regimen in twenty Japanese cancer patients who were concomitantly receiving intravenous granisetron
394 (40 µg/kg on Day 1) and dexamethasone (on Days 1-3).^[48] In this study the reported C_{max} and AUC for the
395 Day 1 of the 125 mg/80 mg dose regimen are 2210 ± 870 ng/mL and 30000 ± 8700 ng·h/mL, respectively,
396 which are slightly higher than those reported for healthy volunteers in the fasted state ($C_{max} = 1003$
397 ng/mL, AUC = 21633 ng·h/mL).^[18,48] In a later study, Bubalo et al. investigated the pharmacokinetics of
398 aprepitant in cancer patients undergoing hematopoietic stem cell transplantation. In this study, fourteen
399 Caucasian patients were administered one 125 mg EMEND® capsule one hour before the first
400 chemotherapy or radiation dose. Ondansetron and dexamethasone (12 mg on Day 1 and 8 mg on the
401 subsequent days) were co-administered prophylactically to all subjects. In this study greater overall
402 variability, as well as the changes in the post-absorptive parameters of the pharmacokinetics of
403 aprepitant were observed. The observed geometric means (range) of key pharmacokinetic parameters
404 were: $t_{max} = 7$ h, $C_{max} = 977$ (741-1289) ng/mL, AUC 27190 (12878-53269) ng·h/mL, CL 0.93 (0.47-1.85)
405 mL/min/kg and V_{ss} 1.54 (1.30-1.84) L/kg. The authors commented that in all subjects the observed V_{ss}
406 was larger than that reported for healthy volunteers and that an altered fraction of unbound drug either
407 in plasma or in tissues could have led to a greater V_{ss} .^[27] The observed discrepancies between the
408 pharmacokinetic parameters reported for healthy volunteers and those reported for cancer patients in
409 the studies of Bubalo et al. and Takahashi et al. may be partly attributable to the co-administration of

410 dexamethasone, which is reported to result in a 30 % increase in the AUC of aprepitant on Day 1, when
411 administered at higher doses,^[7,17] or to the combined effect of all concomitantly administered
412 compounds. Nonetheless, there may be yet other factors, which could also affect the pharmacokinetics
413 of aprepitant in diseased populations. Further data in cancer populations would be needed to reach solid
414 conclusions about the *in vivo* performance of EMEND® in these patients.

415 Last but not least, the relationship between aprepitant pharmacokinetics and its clinical effect should be
416 considered. It has been reported that 80-90 % brain NK-1 receptor occupancy results in significant
417 antiemetic effect, while maximum antiemetic effect is achieved with a greater than 95 % NK-1 receptor
418 blockade.^[17] Furthermore, it has been shown that plasma concentrations of approx. 100 ng/mL produce
419 brain NK-1 receptor occupancy of approximately 90 %.^[7] As previously discussed, the maximum plasma
420 concentrations at the indicated doses (125 mg/ 80 mg dose regimen) can be as high as 1500 ng/mL and
421 the trough levels on the third day of treatment are 600 ng/mL,^[7,17] indicating high receptor occupancy
422 throughout the whole treatment period. Provided there is no lag-phase for achieving the appropriate
423 receptor concentrations, a three-day regimen of 80 mg/ 80 mg, or administration of another formulation
424 that achieves the requisite plasma concentrations is expected to be clinically equivalent to the 125 mg/
425 80 mg dose-regimen. The high dosing compared to the concentrations required to produce efficacy is
426 likely the reason why the regulatory authorities do not consider the differences in the pharmacokinetic
427 data of aprepitant between the fasted and fed state or between healthy volunteers and cancer patients
428 to be clinically significant.

429 **5. Conclusions**

430 The *in vivo* performance of the aprepitant “enhanced” formulation (EMEND® capsules) in healthy
431 volunteers, in both the fasted and fed state, was successfully predicted by coupling *in vitro* data acquired
432 with biorelevant *in vitro* tools with a commercial PBPK modeling platform (the Simcyp Simulator). This
433 study demonstrated the importance of evaluating the effect of gastric residence time as well as the

434 permeability-solubility interplay when predicting the absorption of a poorly soluble API under various
435 dosing and prandial conditions. Using these *in vitro* and *in silico* biopharmaceutical tools, the
436 performance of poorly soluble compounds can be characterized according to a mechanistically-based
437 framework. This approach can support new and generic drug development by promoting rational
438 formulation design and fewer and smaller, but equally robust clinical trials.

439 **Acknowledgments**

440 This work was supported by the European Union's Horizon 2020 Research and Innovation Programme
441 under grant agreement No 674909 (PEARRL), www.pearrl.eu.

442 The authors would like to thank Mr. Fabian Jung and Dr. Anita Nair for their help with the NTA
443 measurements and physicochemical characterization, as well as Dr. Filippos Kesisoglou for the valuable
444 discussions with regard to nanoparticles.

445 **References**

- 446 1. European Medicines Agency - Research and development - PRIME: priority medicines. Available
447 at:
448 http://www.ema.europa.eu/ema/index.jsp?curl=pages/regulation/general/general_content_00
449 [0660.jsp](http://www.ema.europa.eu/ema/index.jsp?curl=pages/regulation/general/general_content_000660.jsp). Accessed February 2, 2018.
- 450 2. Press Announcements - Statement from FDA Commissioner Scott Gottlieb, M.D. on new steps to
451 facilitate efficient generic drug review to enhance competition, promote access and lower drug
452 prices. Available at:
453 <https://www.fda.gov/newsevents/newsroom/pressannouncements/ucm591184.htm>. Accessed
454 February 2, 2018.
- 455 3. Information for Consumers (Drugs) - FDA's Drug Review Process: Continued. Available at:
456 <https://www.fda.gov/Drugs/ResourcesForYou/Consumers/ucm289601.htm#review>. Accessed
457 February 2, 2018.
- 458 4. Parekh A *et al.* Catalyzing the critical path initiative: FDA's progress in drug development
459 activities. *Clin Pharmacol Ther* 2015; 97(3): 221–233. doi:10.1002/cpt.42.
- 460 5. Kalepu S, Nekkanti V. Insoluble drug delivery strategies: review of recent advances and business
461 prospects. *Acta Pharm Sin B* 2015; 5(5): 442–453. doi:10.1016/j.apsb.2015.07.003.
- 462 6. Lipinski CA. Drug-like properties and the causes of poor solubility and poor permeability. *J*
463 *Pharmacol Toxicol Methods* 2000; 44(1): 235–49. Available at:
464 <http://www.ncbi.nlm.nih.gov/pubmed/11274893>. Accessed February 2, 2018.
- 465 7. EMA. EMEND: SUMMARY OF PRODUCT CHARACTERISTICS. Available at:
466 [http://www.ema.europa.eu/docs/en_GB/document_library/EPAR_-](http://www.ema.europa.eu/docs/en_GB/document_library/EPAR_-_)
467 [_Product_Information/human/000527/WC500026537.pdf](http://www.ema.europa.eu/docs/en_GB/document_library/EPAR_-_Product_Information/human/000527/WC500026537.pdf). Accessed October 25, 2017.
- 468 8. FDA-Emend Capsules Pharmacology Review Part 1.pdf. Available at:
469 https://www.accessdata.fda.gov/drugsatfda_docs/nda/2003/21-549_Emend.cfm.
- 470 9. Shono Y *et al.* Forecasting in vivo oral absorption and food effect of micronized and nanosized
471 aprepitant formulations in humans. *Eur J Pharm Biopharm* 2010; 76(1): 95–104.
472 doi:10.1016/j.ejpb.2010.05.009.
- 473 10. Kesisoglou F, Mitra A. Crystalline Nanosuspensions as Potential Toxicology and Clinical Oral
474 Formulations for BCS II/IV Compounds. *AAPS J* 2012; 14(4): 677–687. doi:10.1208/s12248-012-
475 9383-0.
- 476 11. Wu Y *et al.* The role of biopharmaceutics in the development of a clinical nanoparticle
477 formulation of MK-0869: A Beagle dog model predicts improved bioavailability and diminished
478 food effect on absorption in human. *Int J Pharm* 2004; 285(1–2): 135–146.
479 doi:10.1016/j.ijpharm.2004.08.001.
- 480 12. Georgaka D *et al.* Evaluation of Dissolution in the Lower Intestine and Its Impact on the
481 Absorption Process of High Dose Low Solubility Drugs. *Mol Pharm* 2017; 14(12): 4181–4191.
482 doi:10.1021/acs.molpharmaceut.6b01129.

- 483 13. Sjögren E *et al.* *In Silico* Modeling of Gastrointestinal Drug Absorption: Predictive Performance of
484 Three Physiologically Based Absorption Models. *Mol Pharm* 2016; 13(6): 1763–1778.
485 doi:10.1021/acs.molpharmaceut.5b00861.
- 486 14. Söderlind E *et al.* Simulating Fasted Human Intestinal Fluids: Understanding the Roles of Lecithin
487 and Bile Acids. *Mol Pharm* 2010; 7(5): 1498–1507. doi:10.1021/mp100144v.
- 488 15. Takano R *et al.* Rate-limiting steps of oral absorption for poorly water-soluble drugs in dogs;
489 prediction from a miniscale dissolution test and a physiologically-based computer simulation.
490 *Pharm Res* 2008; 25(10): 2334–2344. doi:10.1007/s11095-008-9637-9.
- 491 16. Niederquell A, Kuentz M. Biorelevant Drug Solubility Enhancement Modeled by a Linear
492 Solvation Energy Relationship. *J Pharm Sci* 2018; 107(1): 503–506.
493 doi:10.1016/j.xphs.2017.08.017.
- 494 17. EMEND® Clinical Pharmacology and Biopharmaceutics Review. Available at:
495 https://www.accessdata.fda.gov/drugsatfda_docs/nda/2003/21-549_Emend_biopharmr.pdf.
496 Accessed August 31, 2017.
- 497 18. Majumdar AK *et al.* Pharmacokinetics of aprepitant after single and multiple oral doses in
498 healthy volunteers. *J Clin Pharmacol* 2006; 46(3): 291–300. doi:10.1177/0091270005283467.
- 499 19. Andreas CJ *et al.* In vitro biorelevant models for evaluating modified release mesalamine
500 products to forecast the effect of formulation and meal intake on drug release. *Eur J Pharm*
501 *Biopharm* 2015; 97: 39–50. doi:10.1016/j.ejpb.2015.09.002.
- 502 20. Markopoulos C *et al.* In-vitro simulation of luminal conditions for evaluation of performance of
503 oral drug products: Choosing the appropriate test media. *Eur J Pharm Biopharm* 2015; 93: 173–
504 182. doi:10.1016/j.ejpb.2015.03.009.
- 505 21. Berlin M *et al.* Prediction of oral absorption of cinnarizine – A highly supersaturating poorly
506 soluble weak base with borderline permeability. *Eur J Pharm Biopharm* 2014; 88(3): 795–806.
507 doi:10.1016/j.ejpb.2014.08.011.
- 508 22. Jamei M *et al.* A framework for assessing inter-individual variability in pharmacokinetics using
509 virtual human populations and integrating general knowledge of physical chemistry, biology,
510 anatomy, physiology and genetics: A tale of “bottom-up” vs “top-down” recognition of
511 covariates. *Drug Metab Pharmacokinet* 2009; 24(1): 53–75. Available at:
512 <http://www.ncbi.nlm.nih.gov/pubmed/19252336>. Accessed April 17, 2019.
- 513 23. Cristofolletti R *et al.* Assessment of Bioequivalence of Weak Base Formulations Under Various
514 Dosing Conditions Using Physiologically Based Pharmacokinetic Simulations in Virtual
515 Populations. Case Examples: Ketoconazole and Posaconazole. *J Pharm Sci* 2017; 106(2): 560–
516 569. doi:10.1016/j.xphs.2016.10.008.
- 517 24. Sanchez RI *et al.* Cytochrome P450 3A4 Is the Major Enzyme Involved in the Metabolism of the
518 Substance P Receptor Antagonist Aprepitant Abstract : 2004; 32(11): 1287–1292.
519 doi:10.1124/dmd.104.000216.given.
- 520 25. EMA. EMEND® - Scientific Discussion. 2004; (June): 1–30. Available at:

- 521 [http://www.ema.europa.eu/docs/en_GB/document_library/EPAR_-](http://www.ema.europa.eu/docs/en_GB/document_library/EPAR_-_Scientific_Discussion/human/000527/WC500026534.pdf)
522 [_Scientific_Discussion/human/000527/WC500026534.pdf](http://www.ema.europa.eu/docs/en_GB/document_library/EPAR_-_Scientific_Discussion/human/000527/WC500026534.pdf).
- 523 26. Turner DB *et al.* Prediction of Non-specific Hepatic Microsomal Binding from Readily Available
524 Physicochemical Properties. In: *9th European ISSX Meeting*. Manchester, UK. Available at:
525 <https://www.certara.com/wp-content/uploads/Resources/Posters/DavidISSX2006.pdf>.
- 526 27. Bubalo JS *et al.* Aprepitant pharmacokinetics and assessing the impact of aprepitant on
527 cyclophosphamide metabolism in cancer patients undergoing hematopoietic stem cell
528 transplantation. *J Clin Pharmacol* 2012; 52(4): 586–594. doi:10.1177/0091270011398243.
- 529 28. Rowland M, Tozer TN. *Clinical pharmacokinetics : concepts and applications*. Williams & Wilkins,
530 1995. Available at: https://openlibrary.org/books/OL1101417M/Clinical_pharmacokinetics.
531 Accessed August 7, 2018.
- 532 29. Bergman AJ *et al.* Effect of impaired renal function and haemodialysis on the pharmacokinetics
533 of aprepitant. *Clin Pharmacokinet* 2005; 44(6): 637–647. doi:10.2165/00003088-200544060-
534 00005.
- 535 30. Jamei M *et al.* Population-based mechanistic prediction of oral drug absorption. *AAPS J* 2009;
536 11(2): 225–37. doi:10.1208/s12248-009-9099-y.
- 537 31. Obach RS *et al.* The prediction of human pharmacokinetic parameters from preclinical and in
538 vitro metabolism data. *J Pharmacol Exp Ther* 1997; 283(1): 46–58. Available at:
539 <http://www.ncbi.nlm.nih.gov/pubmed/9336307>. Accessed February 9, 2018.
- 540 32. Andreas CJ *et al.* Mechanistic investigation of the negative food effect of modified release
541 zolpidem. *Eur J Pharm Sci* 2017; 102: 284–298. doi:10.1016/j.ejps.2017.03.011.
- 542 33. Zhou Z *et al.* Statistical investigation of simulated fed intestinal media composition on the
543 equilibrium solubility of oral drugs. *Eur J Pharm Sci* 2017; 99: 95–104.
544 doi:10.1016/j.ejps.2016.12.008.
- 545 34. Kaptay G. On the size and shape dependence of the solubility of nano-particles in solutions. *Int J*
546 *Pharm* 2012; 430(1–2): 253–257. doi:10.1016/j.ijpharm.2012.03.038.
- 547 35. Letellier P *et al.* Solubility of nanoparticles: nonextensive thermodynamics approach. *J Phys*
548 *Condens Matter* 2007; 19(43): 436229. doi:10.1088/0953-8984/19/43/436229.
- 549 36. Tuomela A *et al.* Stabilizing Agents for Drug Nanocrystals: Effect on Bioavailability.
550 *Pharmaceutics* 2016; 8(2). doi:10.3390/pharmaceutics8020016.
- 551 37. Roos C *et al.* In Vivo Mechanisms of Intestinal Drug Absorption from Aprepitant
552 Nanoformulations. *Mol Pharm* 2017; 14(12): 4233–4242.
553 doi:10.1021/acs.molpharmaceut.7b00294.
- 554 38. Fuchs A, Dressman JB. Composition and Physicochemical Properties of Fasted-State Human
555 Duodenal and Jejunal Fluid: A Critical Evaluation of the Available Data. *J Pharm Sci* 2014;
556 103(11): 3398–3411. doi:10.1002/jps.24183.

- 557 39. Bergström CAS *et al.* Early pharmaceutical profiling to predict oral drug absorption: Current
558 status and unmet needs. *Eur J Pharm Sci* 2014; 57(1): 173–199. doi:10.1016/j.ejps.2013.10.015.
- 559 40. Butler JM, Dressman JB. The Developability Classification System: Application of
560 Biopharmaceutics Concepts to Formulation Development. *J Pharm Sci* 2010; 99(12): 4940–4954.
561 doi:10.1002/JPS.22217.
- 562 41. O’Shea JP *et al.* Food for thought: formulating away the food effect - a PEARRL review. *J Pharm*
563 *Pharmacol* 2018. doi:10.1111/jphp.12957.
- 564 42. Hunt JN, Stubbs DF. The volume and energy content of meals as determinants of gastric
565 emptying. *J Physiol* 1975; 245(1): 209–25. Available at:
566 <http://www.ncbi.nlm.nih.gov/pubmed/1127608>. Accessed August 9, 2018.
- 567 43. Cassilly D *et al.* Gastric emptying of a non-digestible solid: assessment with simultaneous
568 SmartPill pH and pressure capsule, antroduodenal manometry, gastric emptying scintigraphy.
569 *Neurogastroenterol Motil* 2008; 20(4): 311–319. doi:10.1111/j.1365-2982.2007.01061.x.
- 570 44. Koziolk M *et al.* Intragastic pH and pressure profiles after intake of the high-caloric, high-fat
571 meal as used for food effect studies. *J Control Release* 2015; 220: 71–78.
572 doi:10.1016/j.jconrel.2015.10.022.
- 573 45. Koziolk M *et al.* Physiological Considerations and In Vitro Strategies for Evaluating the Influence
574 of Food on Drug Release from Extended-Release Formulations. *AAPS PharmSciTech* 2018; 19(7):
575 2885–2897. doi:10.1208/s12249-018-1159-0.
- 576 46. Gore L *et al.* Aprepitant in adolescent patients for prevention of chemotherapy-induced nausea
577 and vomiting: A randomized, double-blind, placebo-controlled study of efficacy and tolerability.
578 *Pediatr Blood Cancer* 2009; 52(2): 242–247. doi:10.1002/pbc.21811.
- 579 47. Ridhurkar DN *et al.* Inclusion complex of aprepitant with cyclodextrin: Evaluation of physico-
580 chemical and pharmacokinetic properties. *Drug Dev Ind Pharm* 2013; 39(11): 1783–1792.
581 doi:10.3109/03639045.2012.737331.
- 582 48. Takahashi T *et al.* Pharmacokinetics of aprepitant and dexamethasone after administration of
583 chemotherapeutic agents and effects of plasma substance P concentration on chemotherapy-
584 induced nausea and vomiting in Japanese cancer patients. *Cancer Chemother Pharmacol* 2011;
585 68(3): 653–659. doi:10.1007/s00280-010-1519-2.
- 586 49. Liu J *et al.* Characterization and pharmacokinetic study of aprepitant solid dispersions with
587 soluplus®. *Molecules* 2015; 20(6): 11345–11356. doi:10.3390/molecules200611345.

588
589

590

Tables

591 *Table 1: Parameter values used for the simulations of the in vivo performance of EMEND® in the fasted*
 592 *and fed states*

Parameters		References and Comments
Dosage form	IR	
Molecular weight (g/mol)	534.44	
Log P	4.8	[9–11,49]
		Estimated using the PE Tool
B/P (Blood/Plasma Coefficient)	1.20	after fitting the available <i>in vivo</i> data (see 2.3.1)
f_u (unbound plasma)	0.02	[7,17,29]
	Absorption	
Absorption Model	ADAM	
Diffusion Layer Model		
Permeability Method		
$P_{eff,man}$ ($\times 10^{-4}$ cm/s)	2.15	Estimated using the PE Tool
Solubility fasted state ($\mu\text{g/mL}$)	13, 30	Stomach, Small Intestine
Solubility fed state ($\mu\text{g/mL}$)	75, 120	Stomach, Small Intestine
	Distribution	
Distribution Model	Minimal PBPK Model with SAC	
SAC Q (L/h)	21.92	Estimated after fitting the
Volume [V_{SAC}] (L/kg)	0.7837	available intravenous <i>in vivo</i> data (see 2.3.1)
V_{ss} (L/kg)	0.875	[7]
	Elimination	
Elimination Type	Enzyme Kinetics	
	$V_{max}=120$ pmol/mg/min	[24]
CYP3A4	$K_m=10.5$ μM	[24]
	$f_{umic}=0.143$	Simcyp Prediction Toolbox
Renal clearance (L/h)	0.0024	[25,28]

593

594

595 *Table 2: Mean (\pm SD) solubility of aprepitant in fasted and fed state biorelevant media at 24 h*

Biorelevant Medium	Solubility ($\mu\text{g/mL}$)	pH _{final}
<i>Fasted state</i>		
Level I FaSSGF	7.62 \pm 0.64	1.6
Level III FaSSGF	5.76 \pm 0.35	1.7
Level I FaSSIF V1	<LOD	6.6
Level II FaSSIF V1	9.87 \pm 2.40	6.5
Level I FaSSIF V3	<LOD	6.8
Level II FaSSIF V3	3.03 \pm 0.06	6.7
<i>Fed state</i>		
Level I FeSSIF V1	<LOD	5.0
Level II FeSSIF V1	53.89 \pm 11.76	5.0
Level I FeSSIF V2	<LOD	5.8
Level II FeSSIF V2	68.58 \pm 6.86	5.8

596

597 *Table 3: Calculated average fold error (AFE) and absolute average fold error (AAFE) for the simulations*
 598 *after oral administration of EMEND® capsules*

Dose	80 mg		125 mg	
	Fasted State	Fed State	Fasted State	Fed State
AFE	1.58	1.31	0.94	1.12
AAFE	1.58	1.44	1.14	1.45

599

600

Figure Captions

601 **Figure 1:** Simulated (thick green line, population mean; dash grey lines, 5th and 95th percentile of
602 population) and clinically reported plasma concentration-time profiles after i.v. administration of 2 mg
603 radio-labelled aprepitant (diamonds), 2 mg radio-labelled aprepitant i.v. concurrently with one 80 mg
604 EMEND[®] capsule (circles) and 2 mg radio-labelled aprepitant i.v. concurrently with one 125 mg EMEND[®]
605 capsule (triangles).^[18]

606

607 **Figure 2:** Mean (\pm SD) % aprepitant dissolved from 80 mg EMEND[®] capsules in: A) Level III FaSSGF (\blacklozenge),
608 Level II FaSSIF V1 (\blacksquare), Level II FaSSIF V3 (\bullet) and B) Level II FeSSGF_{middle} (\times), Level II FeSSIF V1 (\square) and Level
609 II FeSSIF V2 (\circ).

610

611 **Figure 3:** Mean (\pm SD) % aprepitant dissolved from 125 mg EMEND[®] capsules in: A) Level III FaSSGF (\blacklozenge),
612 Level II FaSSIF V1 (\blacksquare), Level II FaSSIF V3 (\bullet) and B) Level II FeSSGF_{middle} (\times), Level II FeSSIF V1 (\square) and Level
613 II FeSSIF V2 (\circ).

614

615 **Figure 4:** Mean (\pm SD) % aprepitant dissolved from: A) 80 mg EMEND[®] capsules and B) 125 mg EMEND[®]
616 capsules, during transfer experiments from Level III FaSSGF (pH =2) to Level II FaSSIF V1 (\blacksquare) and to Level
617 II FaSSIF V3 (\bullet).

618

619 **Figure 5:** Simulated (thick green line, population mean; dash grey lines, 5th and 95th percentile of
620 population) and clinically reported (circles) plasma concentration-time profiles after administration of
621 an: A) 80 mg EMEND[®] capsule and B) 125 mg EMEND[®] capsule, in the fasted state.^[18]

622

623 **Figure 6:** Simulated (thick green line, population mean; dash grey lines, 5th and 95th percentile of
624 population) and clinically reported (circles) plasma concentration-time profiles after administration of
625 an: A) 80 mg EMEND[®] capsule and B) 125 mg EMEND[®] capsule, in the fed state.^[18]

626
627 **Figure 7:** The sensitivity of the simulated profiles after administration of an EMEND[®] 125 mg capsule in
628 the fasted state to variations in the duodenal solubility (i.e. from 10 to 90 µg/mL). The thick line
629 represents the profile using approximately the same solubility value as the one implemented in the
630 currently developed PBPK model.

631
632 **Figure 8:** The sensitivity of the simulated profiles after administration of an: A) 80 mg EMEND[®] capsule
633 and B) 125 mg EMEND[®] capsule, in the fed state to variations in mean gastric residence time (i.e. from 1
634 to 4 h).

635
636 **Figure 9:** The sensitivity of the simulated t_{max} after administration of an: A) 80 mg EMEND[®] capsule and
637 B) 125 mg EMEND[®] capsule, in the fed state to variations in mean gastric residence time (i.e. from 1 to 4
638 h) and permeability values (i.e. P_{eff} from 1.16 to 2.15 x 10⁻⁶ cm/s).

639
640 **Figure 10:** Simulated (thick green line, population mean; dash grey lines, 5th and 95th percentile of
641 population) and clinically reported plasma concentration-time profiles after administration of 125 mg
642 EMEND[®] capsules in fed state. Circles represent the data from Majumdar et al., upon which the PBPK
643 model was based, squares represent the second clinical study conducted by Majumdar et al. to evaluate
644 the pharmacokinetics of the 3-days aprepitant regimen and diamonds represent the study reported by
645 Gore et al.^[18,46]

646
30

647

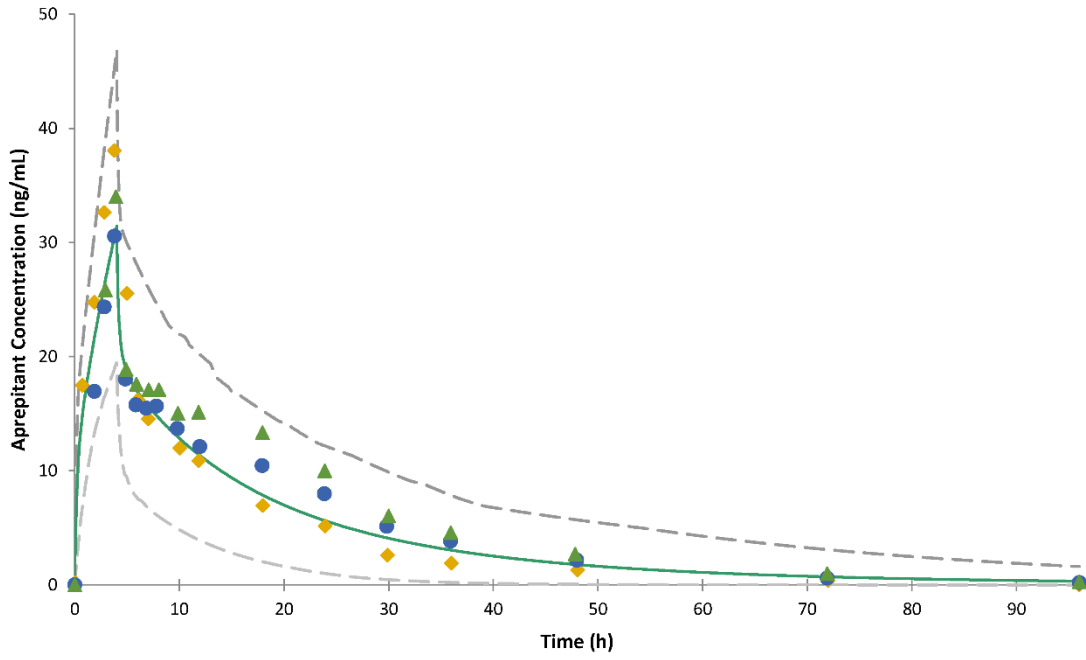
Figures

648

649

Figure 1

650



651

Figure 2

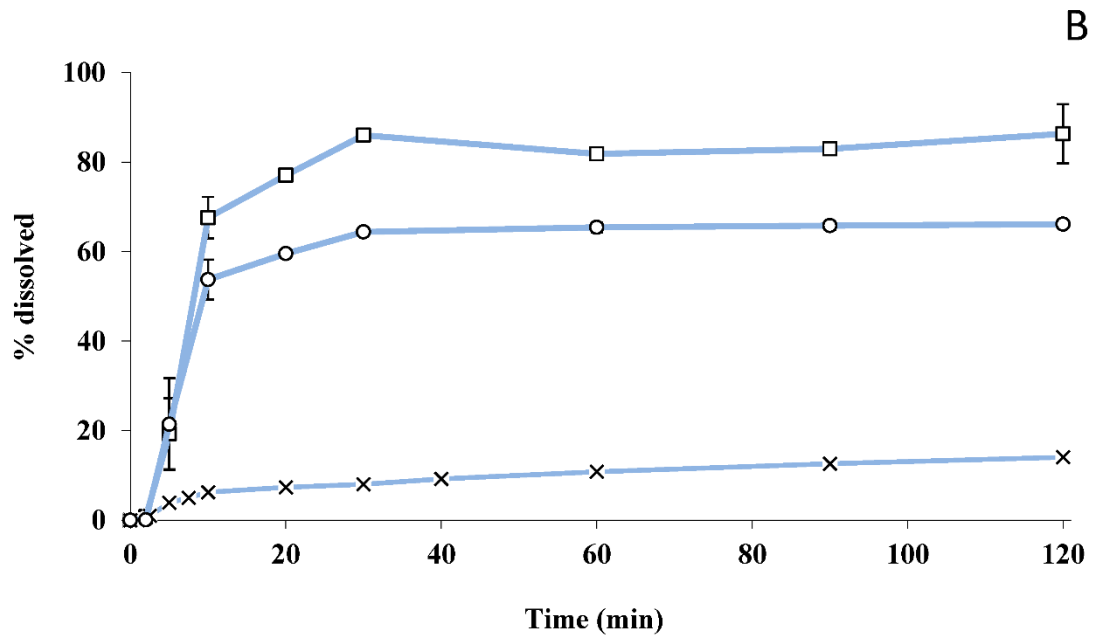
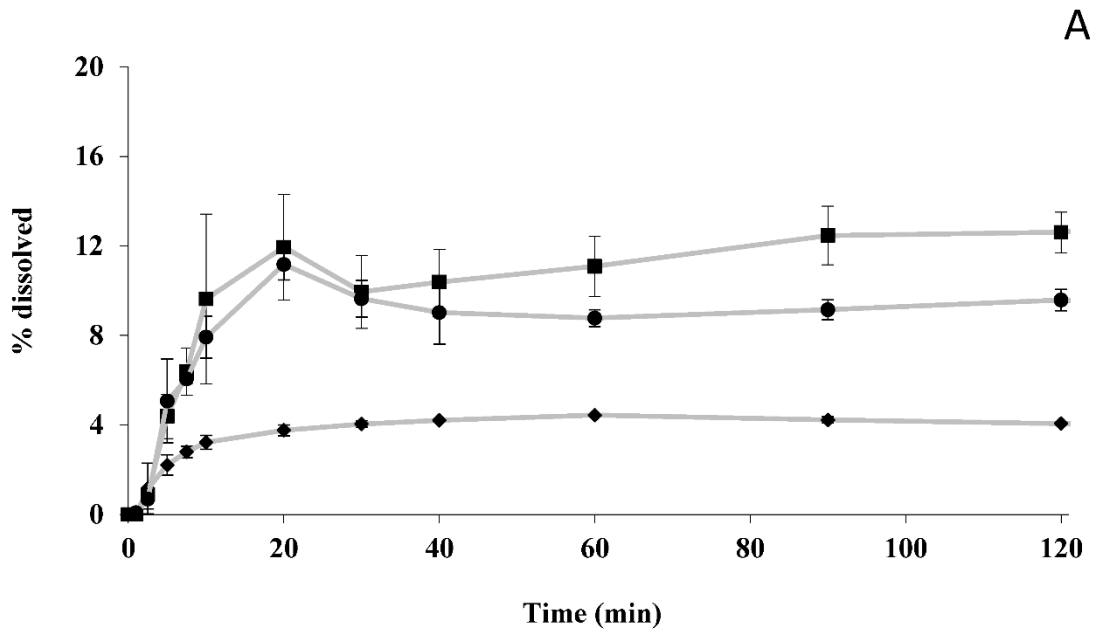


Figure 3

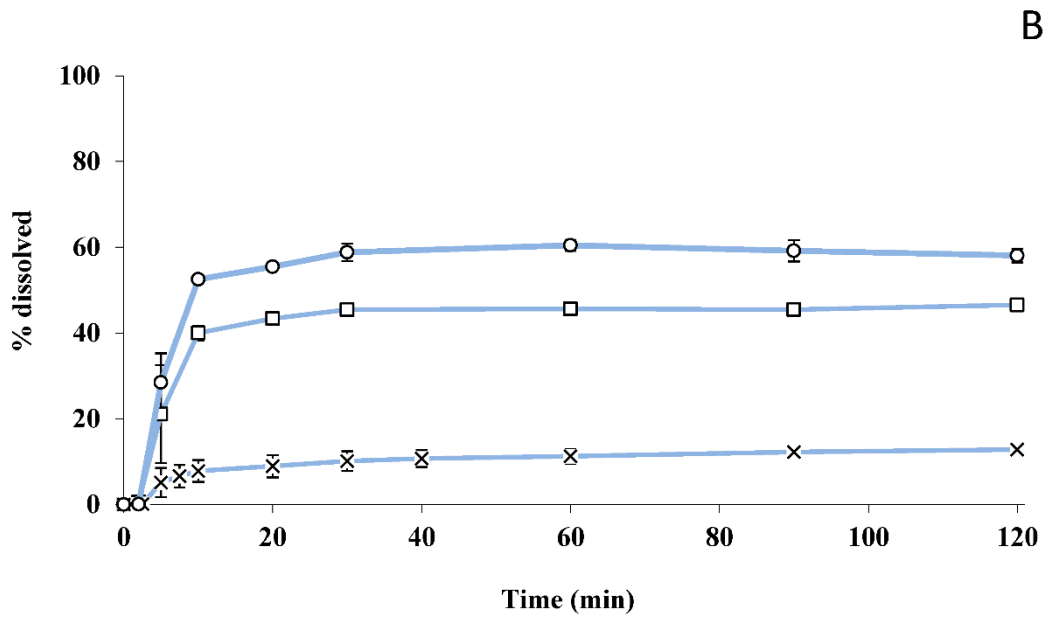
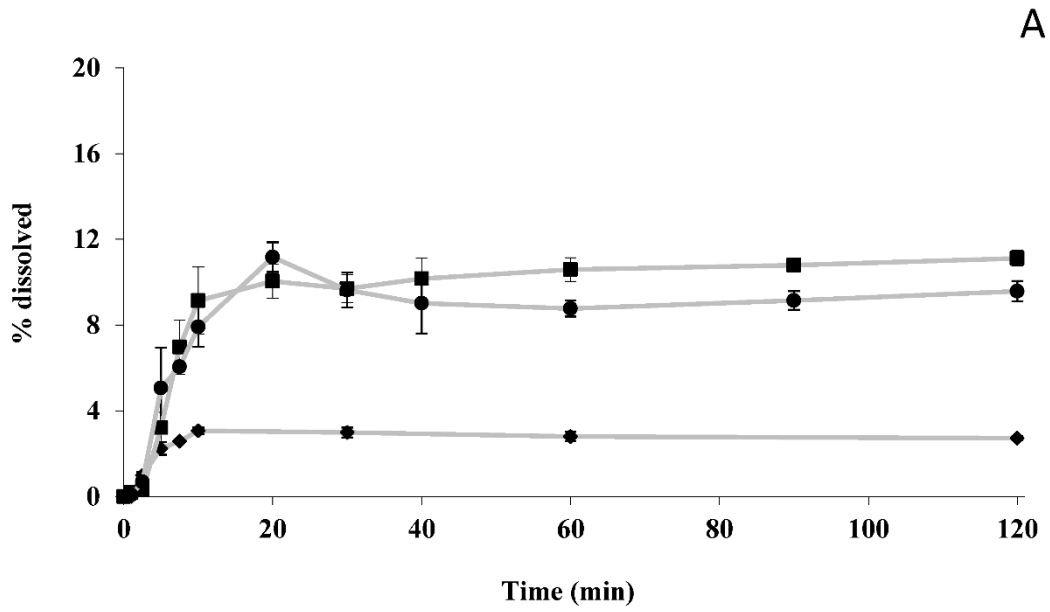
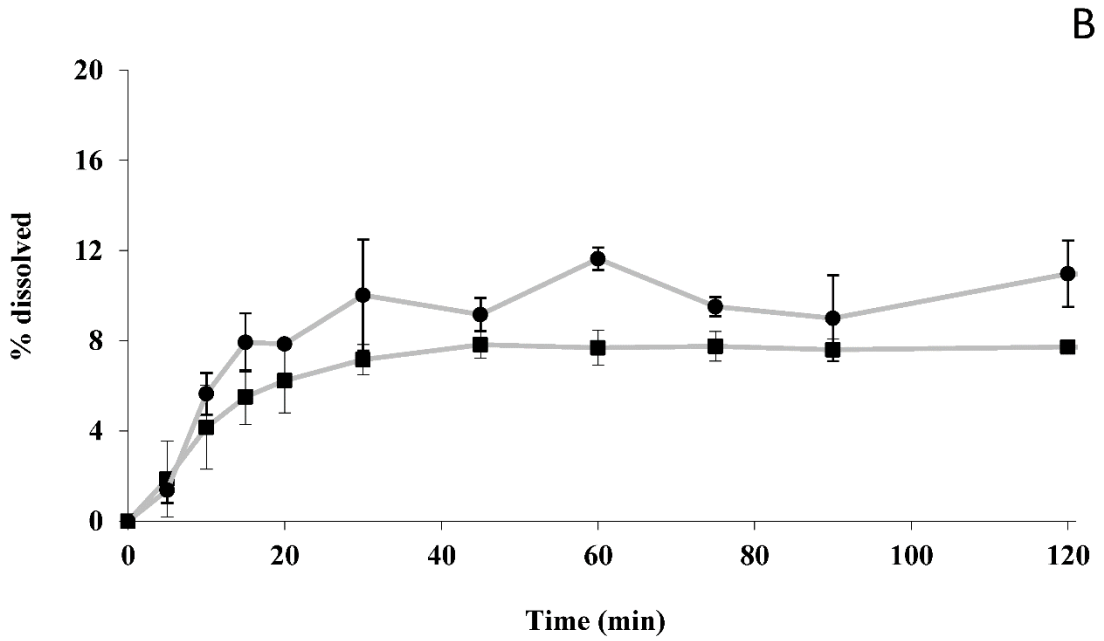
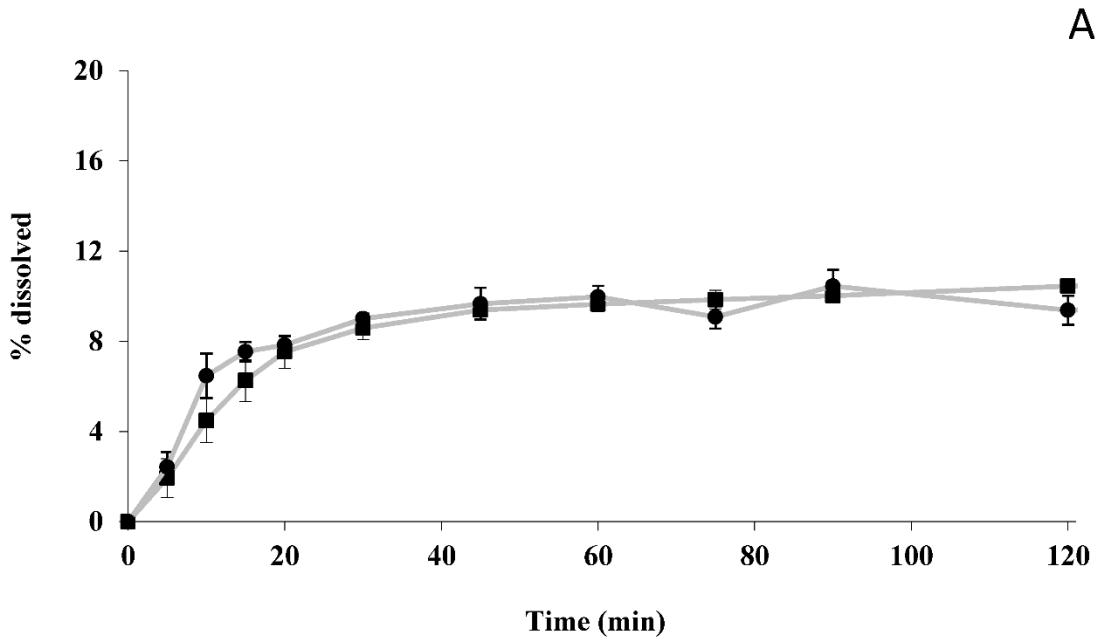


Figure 4



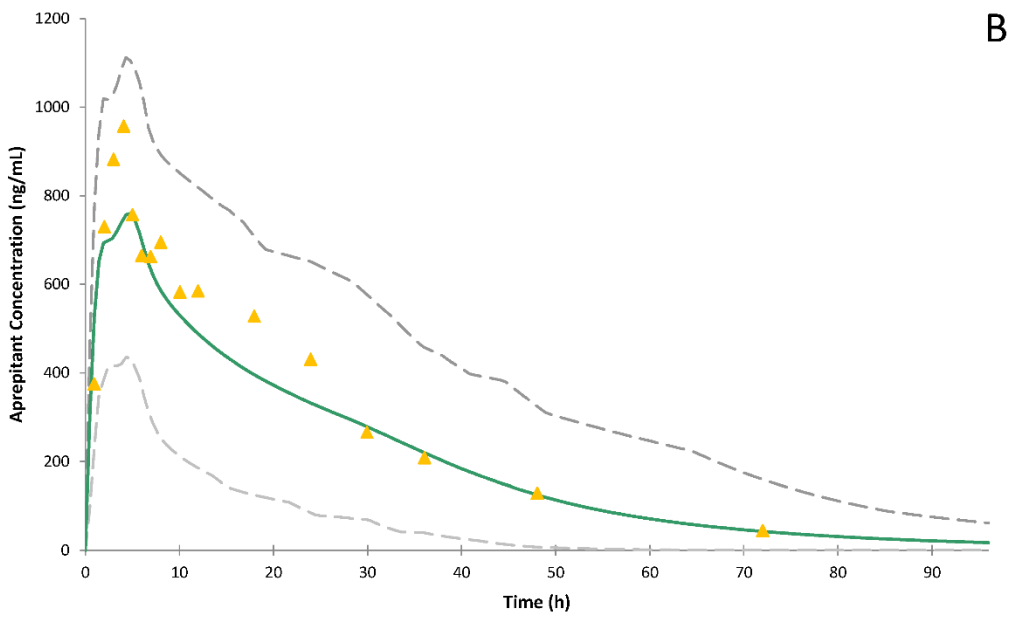
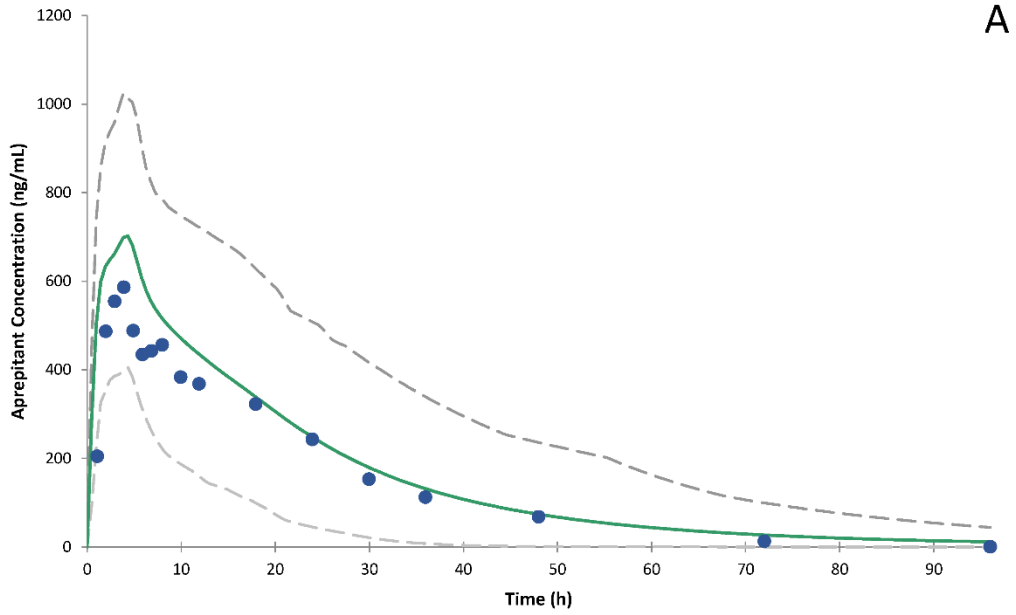
660

661

662

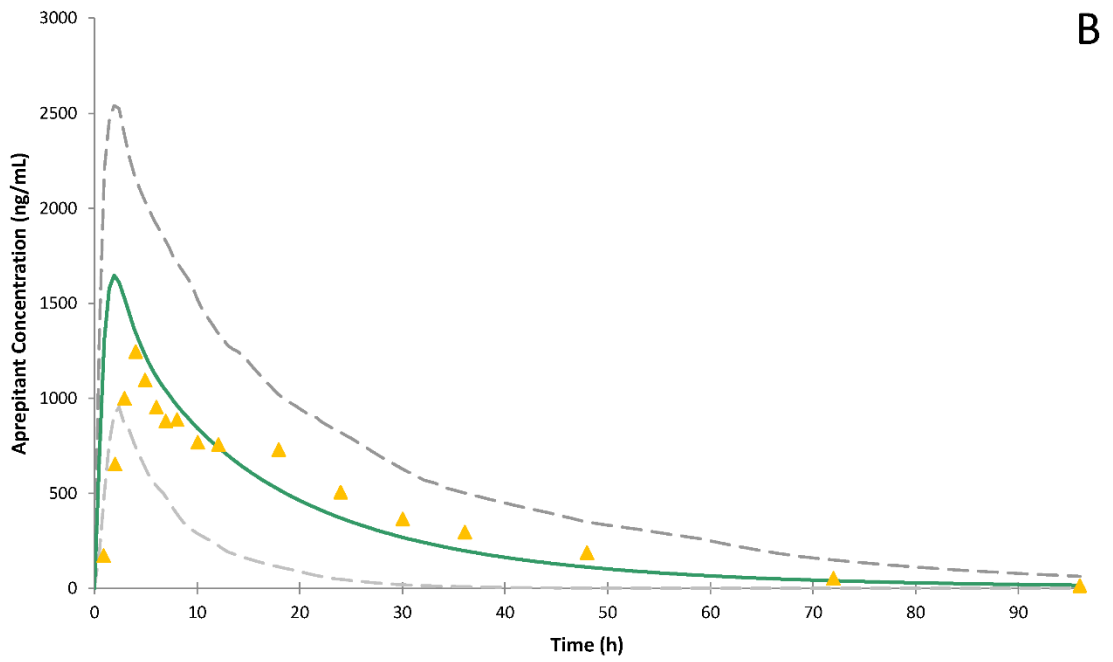
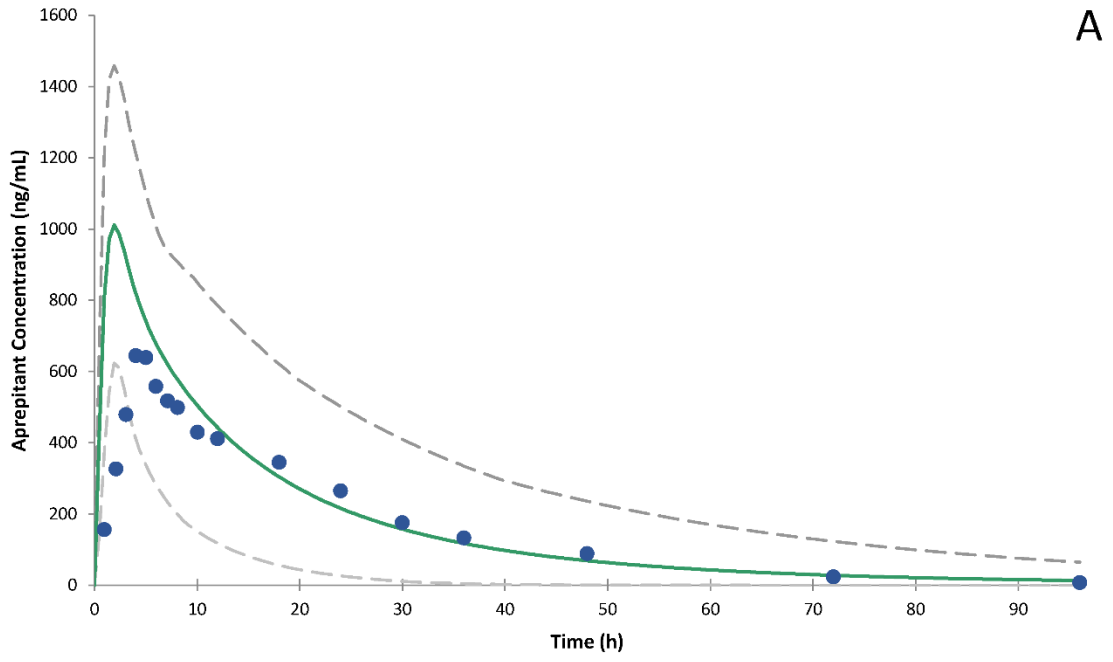
663

Figure 5



667
668

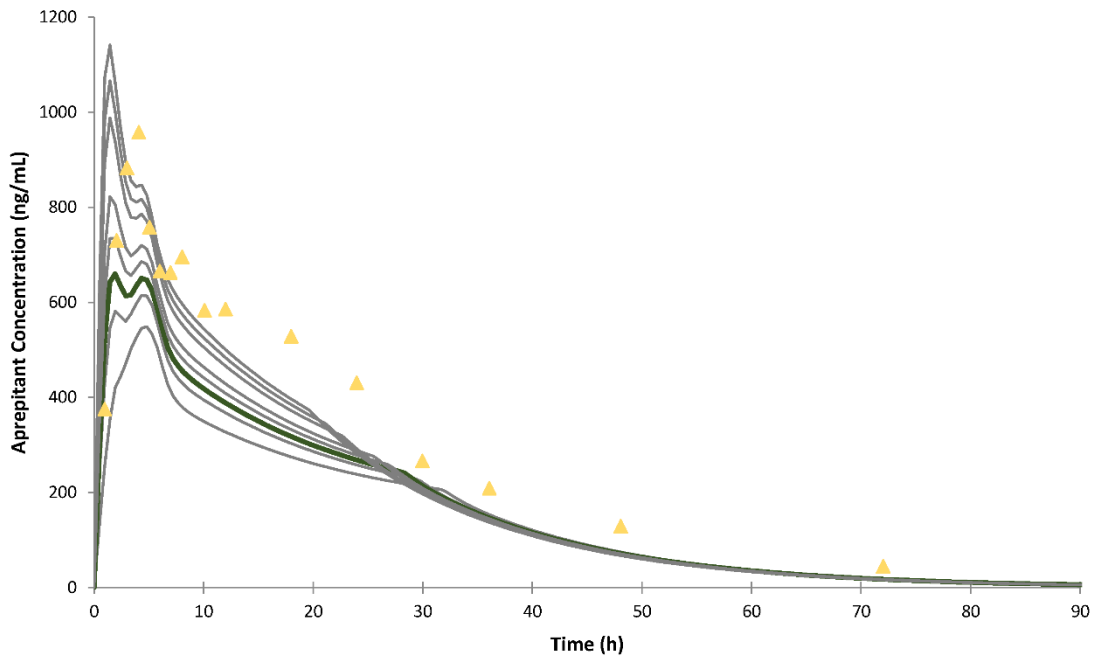
Figure 6



669
670

671

Figure 7

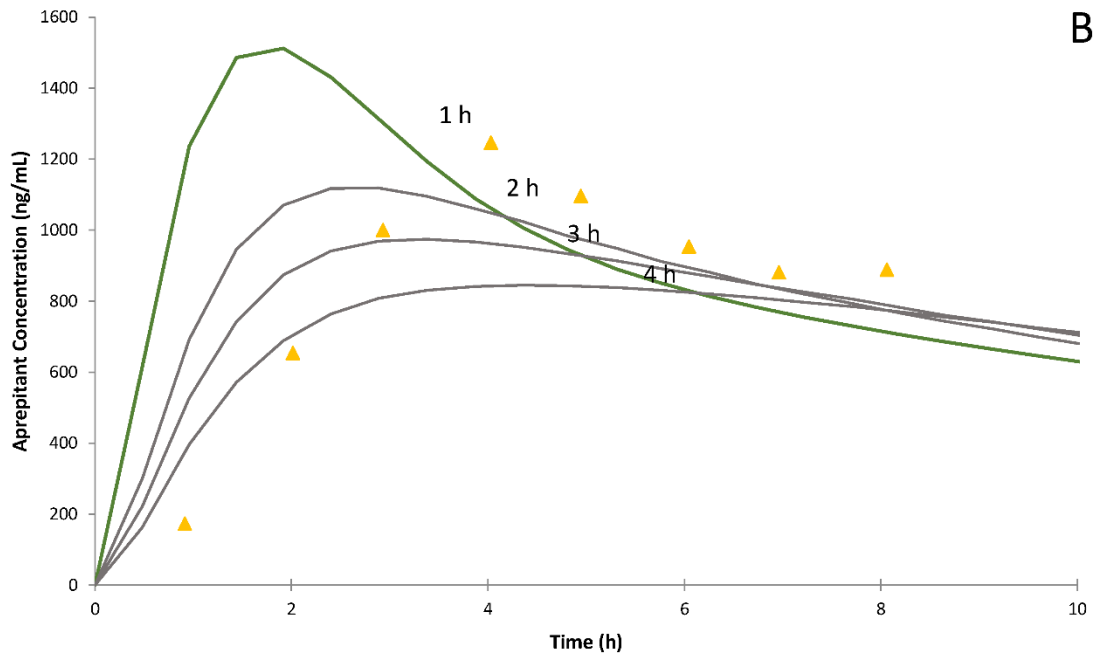
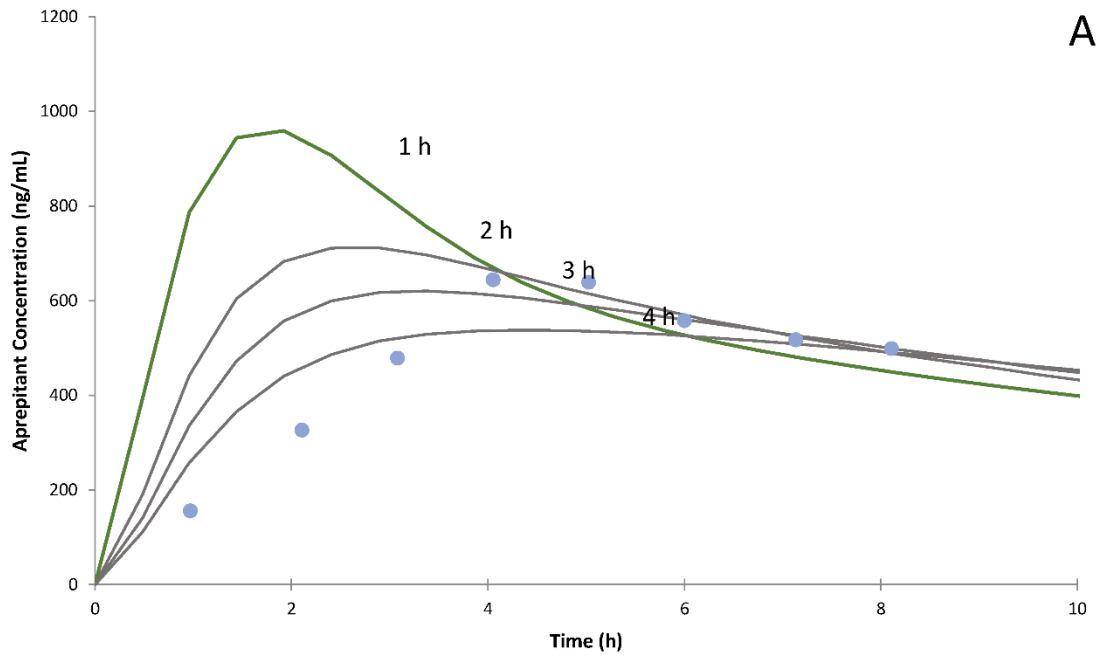


672

673

674

Figure 8



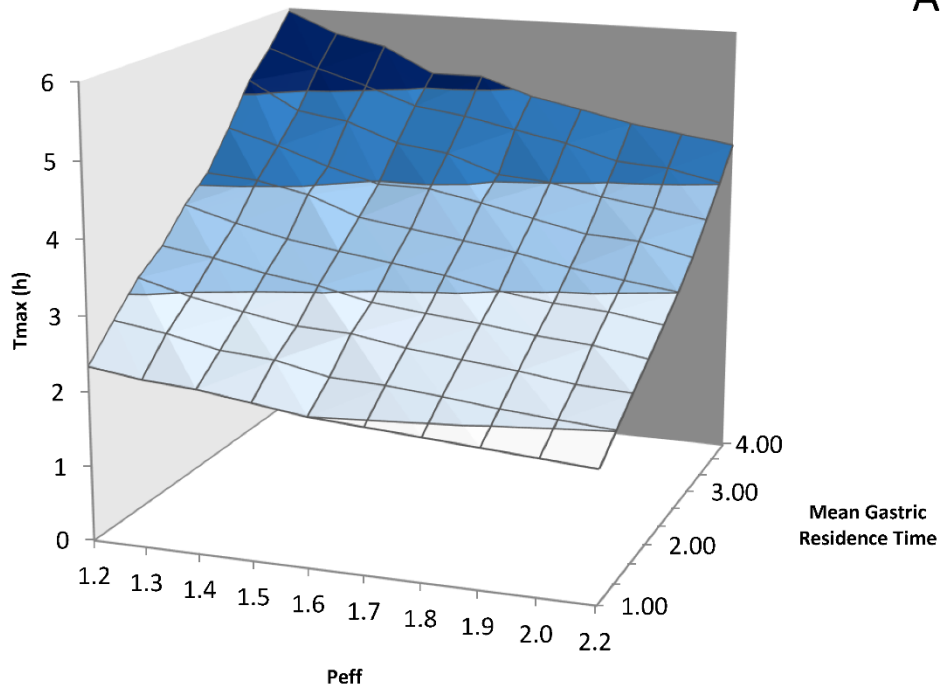
675

676

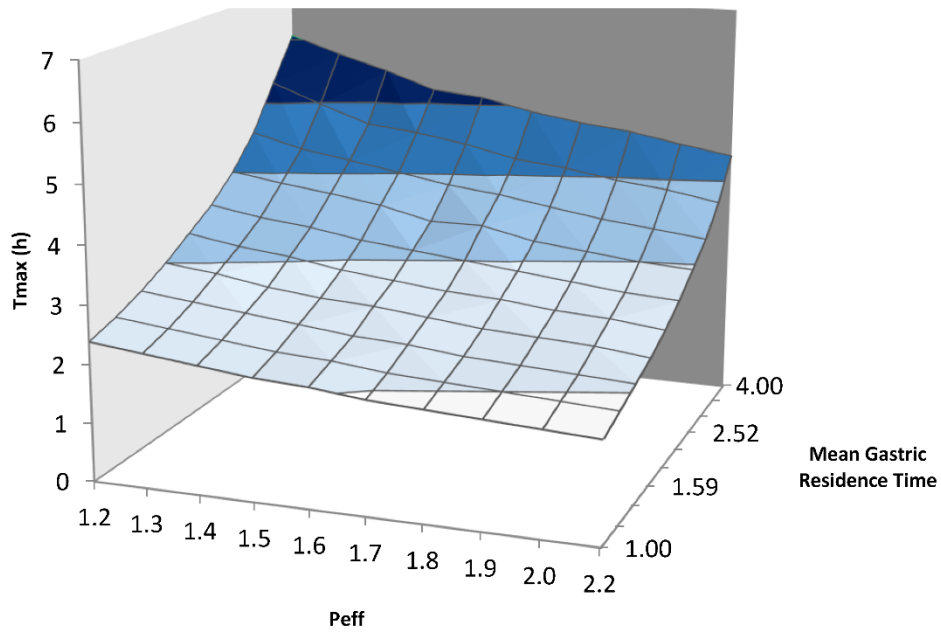
677

Figure 9

A



B

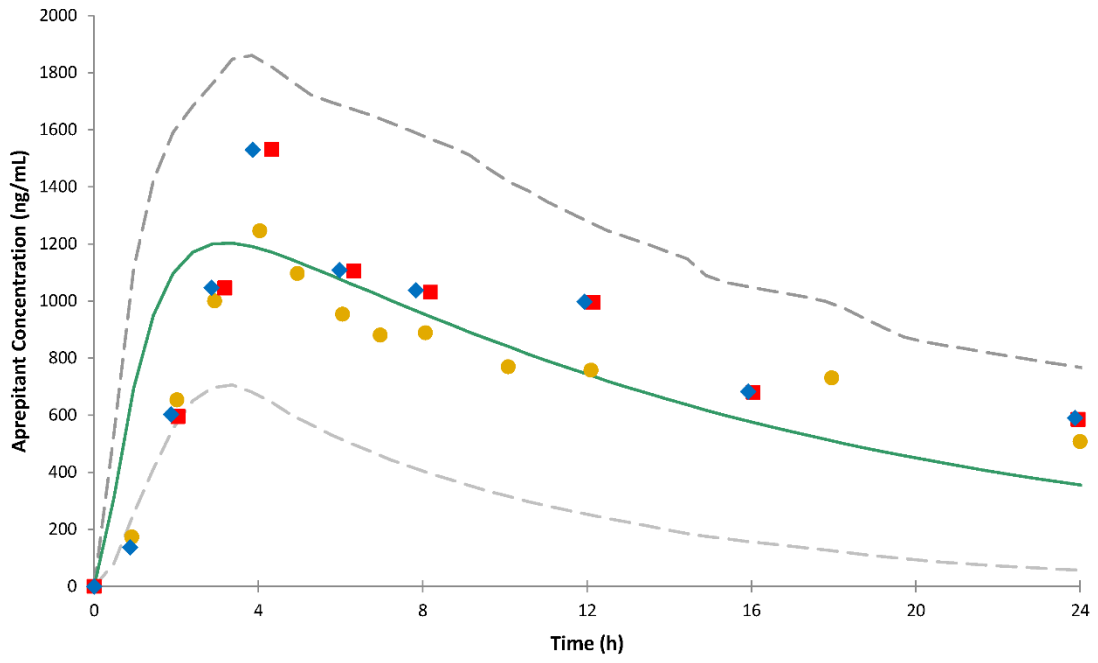


678

679

680

Figure 10



681

682

683